Fossil intermediate-depth earthquakes in subducting slabs linked to differential stress release

Marco Scambelluri[1*], Giorgio Pennacchioni[2], Mattia Gilio[1,5], Michel Bestmann[3], Oliver Plümper[4], Fabrizio Nestola[2]

1 Dipartimento di Scienze della Terra, Ambiente e Vita, University of Genova, Corso Europa 26,16132 Genova, Italy

[2] Dipartimento di Geoscienze, University of Padova, Via G. Gradenigo 6 - 35131- Padova, Italy

[3]GeoZentrum Nordbayern, Friedrich-Alexander University of Erlangen-Nürnberg, Schlossgarten 5, 91054, Erlangen,Germany

[4]Department of Earth Sciences, Utrecht University, Budapestlaan 4, 3584CD Utrecht, The Netherlands

[5] Dipartimento di Scienze della Terra e dell'Ambiente, University of Pavia, Via Ferrata 1, 27100, Pavia, Italy

* corresponding author: marco.scambelluri@dipteris.unige.it

Manuscript n. NGS-2017-02-00378B
Published in Nature Geoscience 27 November 2017, Volume 10; P 960-966
https://doi.org/10.1038/s41561-017-0010-7
Link to publisher version https://www.nature.com/articles/s41561-017-0010-7

The cause of intermediate-depth (50 to 300 km) seismicity in subduction zones is uncertain. It is typically attributed either to rock embrittlement associated with fluid pressurization, or to thermal runaway instabilities. Here we document glassy pseudotachylyte fault rocks – the products of frictional melting during co-seismic faulting – in the Lanzo Massif ophiolite in the Italian Western Alps. These pseudotachylytes formed at subduction-zone depths of 60 to 70 km in poorly hydrated to dry oceanic gabbro and mantle peridotite. This rock suite is a fossil analogue to

oceanic lithospheric mantle undergoing present-day subduction. The pseudotachylytes locally preserve high-pressure minerals indicating an intermediate-depth seismic environment. These pseudotachylytes are important because they are hosted in near anhydrous lithosphere free of coeval ductile deformation, which excludes an origin by dehydration embrittlement or thermal runaway processes. Instead, our observations indicate that seismicity in cold subducting slabs can be explained by the release of differential stresses accumulated in strong, dry, metastable rocks.

Over a total length of ~55,000 km, subduction zones at convergent plate margins are the main setting for earthquakes globally. In such environments, seismicity is caused by accumulation and release of stress from shallow levels down to intermediate depths (50-300 km)[1-3]. Intermediate-depth earthquakes are inaccessible to direct investigation and much knowledge relies on seismic data, rock-deformation experiments and modelling. Geophysical data show that the seismic activity in subduction zones concentrates either inside the subducting lithosphere, or in kilometres-thick layers along the plate interface. These layers consist of hydrated rocks hosting pressurized pore fluids and show low seismic velocities[4-7]. Experimental work and numerical models suggest that subduction-zone seismicity is triggered by a thermal runaway instability[8-12], dehydration embrittlement[2,13-14], phase transformation[15] or reactivation of earlier discontinuities[1]. To date, investigations have prevalently focused on seismicity in the subducting oceanic crust and in the low-velocity plate-interface[2,4,5,13-15], whereas the seismic potential of lithospheric mantle of subducting oceanic plates remains poorly understood.

Compared to the above studies, field-based investigations of exhumed high-pressure rocks have so far been under-utilised to directly study fossilised earthquake phenomena. Pseudotachylytes, the solidified friction-induced melts produced during seismic slip along a fault, are unique indicators of paleo-earthquakes in exhumed faults. Unfortunately, pseudotachylytes are rarely preserved in the rock record and the examples related to subduction settings are limited to findings within exhumed blueschist- and eclogite-facies continental and oceanic crust sections[16-22].

Here we investigate pseudotachylytes in a gabbro-peridotite body from the Lanzo Massif (Italian Western Alps), a tectonic slice of oceanic mantle involved in Alpine subduction. These pseudotachylytes were previously attributed to a pre-subduction oceanic detachment setting[23,24], but here we conclude they formed under eclogite-facies conditions. Although similar to pseudotachylytes from Corsica, related to blueschist-facies metamorphism at shallower subduction depths[19-22,25], our case study provides a unique record of oceanic slab eclogitization in the Wadati-Benioff seismic zone, in analogy with the intermediate-depth seismicity affecting the lithospheric mantle in present-day subducting slabs.

The host-rocks of fossil seismic faults

The Alpine Lanzo Massif is a 20x9 km-wide sliver of oceanic mantle peridotite with subordinated 160 Ma old gabbro dykes[23], regionally embedded in serpentinite and metagabbro (Supplementary Fig. S1). It records oceanic serpentinization around unaltered peridotite cores[26] and later subduction-related Alpine metamorphism under eclogite-facies conditions (2-2.5 GPa and 550-620 °C at 55-46 Ma)[26-29]. The southernmost body of the Lanzo Massif (Moncuni, Fig. S1) has a core of poorly hydrated to anhydrous mantle peridotite and pyroxenite intruded by cm- to 10's of cm-thick dykes of preserved dry gabbro. Such unaltered gabbro and peridotite are predominant in Moncuni, and contain minor volumes (~5vol%) of hydrated metaperidotite and metagabbro that record static, eclogite-facies metamorphism. The heterogeneous water distribution can be related to limited oceanic hydration prior to subduction. Unaltered and hydrated-eclogitized domains form a coherent body that underwent the same subduction-zone evolution, but the predominant peridotite and gabbro metastably escaped eclogitization. Hence, most oceanic lithosphere in Moncuni, as in the whole Lanzo Massif, metastably preserved the pristine structures and mineral assemblages representative of pre-subduction mantle and oceanic settings throughout its 100 Myr-long history. Very limited water access during the entire evolution thus prevented the metamorphic re-equilibration of poorly hydrated to anhydrous rock domains and ductile deformation of entire rock mass during subduction.

The unaltered peridotite comprises olivine, orthopyroxene, clinopyroxene and spinel showing a coarse, pre-oceanic, mantle tectonite foliation[23]. This rock is enriched in plagioclase due to melt-rock reaction during mantle-to-ocean evolution[23] and, in addition, can display minor amounts of amphibole[23] and serpentine. The unaltered gabbro dykes display igneous clinopyroxene, olivine and plagioclase, locally overprinted by an oceanic high-temperature (700-800 °C) mylonitic foliation[24] (Supplementary Information 1, Fig. S2). The high-temperature, pre-subduction, mantle-to-oceanic foliations are the only ductile deformation structures developed in these rocks.

In the Moncuni eclogitic metaperidotite, mantle olivine and plagioclase were replaced by metamorphic olivine + antigorite, and by zoisite + garnet + chloritoid + chlorite, respectively (Fig. 1a,b). In eclogitic metagabbros, igneous plagioclase was overgrown by jadeite + zoisite ± garnet ± kyanite, olivine by talc ± tremolite and clinopyroxene by omphacite; chloritoid coronas formed between pseudomorphosed plagioclase and olivine. Such transformations are typical of Alpine eclogitic metagabbros and metaperidotites[26-30].

Relative timing and pressure-temperature earthquake faulting conditions

Numerous pseudotachylyte veins crosscut the Moncuni peridotite, pyroxenite and gabbro, the derived high-temperature tectonite and mylonite, and the eclogitic metaperidotite and metagabbro. Pseudotachylytes occur as moderately to steeply dipping fault veins, striking N-S to NW-SE, trending subparallel to the gabbro dykes but also locally crosscutting the dykes. The pseudotachylyte fault veins are associated with sub-parallel, pervasive, sharp, brittle slip planes and thin cataclasites, all crosscutting the pre-existing tectonitic (peridotite), magmatic and mylonitic (gabbro) fabrics. Pseudotachylytes in rocks hosting even trace amounts of water (poorly hydrated peridotite, eclogitic metaperidotite and metagabbro) do not contain glass, but a crypto- to micro-crystalline matrix. Glass is only preserved in pseudotachylytes within dry, unaltered gabbros. The thickest pseudotachylyte veins (a few 10's of cm, Fig. 2a) occur in peridotite: the matrix and microlites entirely annealed to an aggregate of olivine, orthopyroxene, clinopyroxene and Cr-spinel (Fig. 2b). This agrees with previous description of orthopyroxene, olivine, interstitial clinopyroxene and spinel microlites in such pseudotachylytes[23,24], and suggests cooling and post-cooling recrystallization of the frictional melt in the spinel stability field for ultramafic systems.

In gabbros, mylonitic gabbros (Supplementary Information 1, Fig. S2) and eclogitic metagabbro (Fig. 2c), pseudotachylyte fault and injection veins are few microns- to a few millimetres-thick. In gabbros and gabbro mylonites the rock-forming minerals display a pervasive shattered microstructure and brittle comminution close to microfaults and pseudotachylytes, and occur as unreacted clasts within cataclasites (Supplementary Information 1, Figs. S3, S4) and pseudotachylytes. Pseudotachylyte fault and injection veins cut the cataclastic zones and truncate all minerals (Supplementary Information 1, Figs. S5, S6). Other than a cataclastic flow structure, the wall-rock minerals aside faults and pseudotachylytes do not show evidence of progressive grain-size reduction by dynamic recrystallization (Supplementary Information 1, Figs. S5,S6). In pristine gabbros, pseudotachylytes consist of glass including microlites of clinopyroxene, plagioclase, garnet and fragments of the host rock that lack kinking and foliation planes. Figure 3a shows two glassy pseudotachylyte fault veins with protruding injection veins cutting a gabbro. The larger vein shows a flow layering with a band of pure glass (white dotted line, Fig. 3a) and a band of clast-laden glass clustered with plagioclase and clinopyroxene microlites (a few μm sized). Microlites also occur in trails along healed microcracks confined within the pseudotachylyte. Raman analysis shows the pseudotachylyte glass is anhydrous (Supplementary Information 1, Fig. S7). Micrometric pyrope-rich garnet associates with plagioclase and clinopyroxene microlites (Figs. 3b-d; Supplementary Information 1, Fig. S8). Garnet also occurs in rare, few μm-wide, discontinuous coronas at plagioclase-olivine boundaries only in the gabbro wall-rocks adjacent the pseudotachylyte veins (Fig. 3a). This corona-garnet acted as nucleation site for garnet microlites that overgrew the pseudotachylyte glass (Fig. 3e). Pseudotachylyte in pyroxenite contains pyrope-rich garnet microlites with dendritic shape suggesting growth from quenched frictional melts[31,32] (Figs. 3f, S9). In unaltered gabbro, garnet is thus restricted to pseudotachylytes and grew either inside the veins, or in the adjacent wall-rock. The major element compositions of such garnets are all comparable with those of eclogitic garnet from other Alpine gabbros with similar bulk composition (Supplementary Information 1, Fig. S10). This helps bracketing pseudotachylyte formation within a stage of high-pressure garnet growth.

The eclogitic metagabbro and metaperidotite domains at Moncuni are limited in volume, but their relationships with pseudotachylyte are fundamental for assessing the tectonic environment of seismic faulting. Figure 4a shows pseudotachylyte veins and sub-parallel microfaults dissecting the contact between metagabbro and metaperidotite. Within the metagabbro, these microfaults offset cataclastic igneous pyroxene cemented by omphacite (Fig. 4b) and cut the jadeite + zoisite pseudomorphs after plagioclase (Fig. 4a). The microfaults contain clastic fragments of jadeite and zoisite replacing plagioclase and are overgrown by eclogite-facies dendritic garnet (Supplementary Information 2, Figs. S12-S14, garnet composition in Fig. S10). Garnet growth near pseudotachylytes and microfaults was likely enhanced by the thermal transient caused by frictional heating.

In metaperidotite, the pseudotachylyte matrix consists of olivine and pyroxene microlites variably altered to serpentine, talc and tremolite. These pseudotachylytes cut prograde antigorite veins (Supplementary Information 2, Fig. S15) and include: (1) clasts of mantle olivine overgrown by high-pressure metamorphic olivine; (2) olivine clasts hosting antigorite veinlets truncated against the pseudotachylyte (Figs. 4c,d); (3) high-pressure pseudomorphs after mantle plagioclase corroded by the pseudotachylyte melt (Fig. 4d; Supplementary Information 2, Fig. S16). Olivine microlites display higher Mg concentrations than the host-rock olivine (Supplementary Information 2; Fig. S17). Late-stage veins cutting metagabbro, metaperidotite and pseudotachylyte (Fig. 4a) display high-pressure mineralogy: the same vein contains zoisite+chlorite+omphacite in the metagabbro and talc+tremolite in the ultramafic pseudotachylyte (Supplementary Information 2, Figs. S18a-c). Pseudotachylyte and microfaults thus cut eclogitized metagabbro and metaperidotite (Fig. 4), and are in turn overgrown by eclogitic garnet and cut by high-pressure veins (Figs. S12,S18).

Pressure-temperature estimates for Lanzo eclogitic metagabbros[28] yield 2-2.5 GPa and 550-620 °C, corresponding to a 8 °C/km gradient similar to that of modern subduction zones[33]. In metaperidotite, formation of secondary olivine via reaction antigorite + brucite = olivine + fluid[26,30] and breakdown of mantle plagioclase to chlorite, zoisite, garnet occurred at comparable conditions of 2-2.5 GPa and 600 °C[26]. Pressure-temperature estimates done for the Moncuni hydrated-eclogitized metagabbro and metaperidotite yield similar values. We calculated mineral phase stabilities using the hydrated-eclogitized rock compositions, because they represent the only water-saturated reactive volumes that equilibrated under eclogite-facies conditions. Maximum 2.2 GPa and 600 °C are achieved for crystallization of omphacite, zoisite, garnet and kyanite after the gabbro plagioclase (Supplementary

Information 2, Fig. S18d). Formation of talc+tremolite in veins cutting the ultramafic pseudotachylyte occurred below 2.2 GPa (Supplementary Information 2, Fig. S18e).

In gabbros, the pyrope content of the garnet microlites and eclogitic garnet growth after the pseudotachylyte glass (Fig. 3e) suggest that faulting occurred at ~70 km depth (Fig. S18d,e). In eclogitized rocks, the omphacite-cemented breccia (Fig. 4b), entrainment of eclogitic mineral clasts in pseudotachylyte and microfaults (Figs. 4c,d), eclogitic garnet overgrowth of microfaults in metagabbro (Supplementary Information 2, Figs. S12-S14), and high-pressure veins cutting pseudotachylytes, all suggest eclogite-facies, intermediate-depth seismic faulting.

Potential mechanism for intermediate depth seismicity

The Moncuni pseudotachylyte occurs in ophiolitic gabbro-peridotite recording pre-subduction high-temperature ductile deformation during mantle flow and oceanic mylonitization[23,24]. We did not observe any crystal-plastic flow referable to subduction (Supplementary Information 1, Fig. S6). All studied rocks display either mantle tectonite fabrics, or gabbroic igneous and mylonitic oceanic textures. The entire Alpine subduction-zone recrystallization took place statically and produced pseudomorphic and coronitic textures (Figs. 1a, 2c, 4a; Supplementary Information 2, Fig. S11). All rocks escaped ductile deformation (and locally metamorphism) during subduction, when co-seismic rupture and frictional melting took place. The mechanical response, the metastable survival of pre-subduction mineral assemblages and the preservation of dry pseudotachylyte glass imply this rock package experienced very limited hydration. Our observations highlight the intimate link between seismic activity and strong, poorly hydrated, metastable sections of subducted oceanic lithosphere. This allows constraining the seismogenic environment and discussing the mechanism triggering the intermediate-depth seismicity recorded at Moncuni.

Thermal runaway and dehydration embrittlement are the most accredited earthquake mechanisms by geoscientists. Present-day intermediate-depth earthquakes in the mantle have been related to thermal runaway[34,35]. This mechanism explains the syn-kinematic association of pseudotachylyte and mylonites: in blueschist-facies gabbro-peridotite from Corsica, pseudotachylyte was synchronous with mylonitization of the wall-rocks. This is indicated by (1) foliation development and grain-size reduction via dynamic recrystallization in rock domains near fault planes, and by (2) entrainment of deformed wall-rock fragments in pseudotachylyte veins[21,22]. Such evidence enabled linking faulting to localized crystal-plastic deformation and thermal runaway under stress up to 580 MPa or more[21,22,36]. Moncuni pseudotachylytes invariably cut pre-subduction foliated peridotite and gabbro, as well as undeformed, massive rocks. Absence of an eclogite-facies mylonitic foliation and of dynamic recrystallization in the selvages of the fault veins, and a lack of foliated eclogitized rock fragments inside pseudotachylytes suggest that Moncuni, different from Corsica, does not record crystal-plastic deformation precursory to seismic slip. The dry glass composition moreover indicates that little water was available to promote ductile shearing[11]. Overall, the above features suggest that frictional melting at Moncuni was not caused by thermal runaway shear instability.

Regarding dehydration-induced seismic embrittlement, laboratory experiments that investigated behaviour of dehydrating serpentinite by monitoring of acoustic signals provide contrasting results. Whereas some experiments report that serpentine dehydration produces acoustic emissions[13,37], others show that dehydration occurs without embrittlement and acoustic activity[38,39]. Recent deformation experiments on dehydrating synthetic aggregates of antigorite + olivine show that acoustic emissions associated with shear failure can occur in samples containing small amounts of antigorite (5vol%)[40]. These results show that little dehydration is necessary to trigger seismicity and suggest that dehydration-induced stress transfer, rather than fluid overpressure, causes embrittlement[40]. Comparably, Moncuni hosts ~5vol% hydrated metaperidotite recording initial antigorite dehydration to secondary olivine (Fig. 1a), producing only 2wt% fluid from fully serpentinized rocks[30]. The amount of water released by the volumetrically subordinate metaperidotite is thus insufficient to induce extensive seismic faulting in the whole Moncuni body. The presence of metamorphic olivine clasts within the pseudotachylyte (Fig. 4c) may even suggest that antigorite dehydration predated the seismic activity. The Moncuni eclogitic metagabbro does not contain amphibole and/or lawsonite (whose dehydration is suggested to cause seismic embrittlement in the crustal section of subducting slabs[14]), and the crosscutting cataclasite and microfaults entrain zoisite clasts that are stable during the eclogite-facies event (Supplementary Information 2, Figures S12, S13). Consequently, rock embrittlement due to fluid overpressure does not represent a viable mechanism to explain seismicity at Moncuni. Instead, as achieved in deformation experiments[40], shear failure may have occurred in strong peridotite (and gabbro) hosting minor, dehydrating, antigorite domains. As suggested by the experimental modelling[40], dehydrating antigorite domains lost their load capacity and transferred stress to the surrounding peridotite, inducing instability and faulting in the olivine-rich rock asperities[40]. Stress propagation out of minor dehydrating metaperidotite volumes, or from serpentinite enclosing the Moncuni body, into unaltered peridotite and gabbro may thus explain formation of the observed pseudotachylytes.

Moreover, the pressure-temperature conditions of Moncuni pseudotachylyte formation (Supplementary Information 2, Figs. S18d,e) coincide with the depth of plate unbending[41]. This process could also have contributed to enhanced differential stress in the uppermost part of the strong dry slab which might have exceeded the stress needed for peridotite failure (580 MPa)[36].

Locating the seismic hypocenter

The distribution of intermediate-depth seismicity in subduction zones shows that seismic events nucleate in low-velocity zones at the plate interface[4,42-45], and inside the subducting plate, in the upper Wadati-Benioff zone[4,5,42-45]. The low-velocity zones can consist of (1) altered crustal sections of the slab[5], (2) mélanges of rocks derived from both the subducting slab and overriding plate[5], and (3) large serpentinite slices detached from the slab[46]. Seismic wave velocities in these domains are hampered by the presence of abundant hydrous minerals and pressurized fluids[6,7], which make them preferential sites for seismic dehydration embrittlement[2,13-14] and non-volcanic tremors[47]. In contrast, the Wadati-Benioff seismic zone can be located inside the lower oceanic crust or in the upper lithospheric mantle of subducting plates[5]. In this deeper seismic level, heterogeneous hydration of mantle rocks can be localized along earlier oceanic detachment faults and/or extensional faults developed during slab bending in the outer rise of subduction zones[48].

Figure 5 helps identifying the seismic subduction-zone environment for the Moncuni pseudotachylytes. Moncuni, like the entire Lanzo Massif, differs from the other Alpine ophiolitic complexes, which pervasively equilibrated to high-pressure metamorphic assemblages during subduction[49]. These complexes either derived from the altered upper part of oceanic slabs, or from plate interface domains, where extensive metamorphic re-equilibration occurred in presence of abundant fluids. Pseudotachylytes were not observed hitherto in serpentinite and other hydrated eclogite-facies rocks, whose potential seismic record is represented by eclogitic breccias[50] related to high fluid pressures. In contrast, the dry and metastable Moncuni and Lanzo peridotite fits a location in the intra-slab lithosphere (Fig. 5a), whose structures and behaviour correspond to the available descriptions of eclogitic pseudotachylyte in metastable, dry rocks[16-17,31-32]. We thus conclude that strong dry to poorly hydrated peridotite and gabbro within subducting slabs can either undergo stress transfer from nearby dehydrating rock domains[40], or accumulate large differential stress during plate unbending[41], which may represent alternative mechanisms to generate intermediate-depth seismicity in subduction-zone environments.

Acknowledgements

We greatly benefitted from discussions with P. Agard, T. Ferrand, A. Schubnel, O. Onken, E. Cannaò, S. Poli and from constructive comments by T.B Andersen and two anonymous reviewers. We thank M. Kendrick for revising the pre-submission manuscript, A. Risplendente and L. Negretti for technical assistance during SEM and WDS-microprobe work. M.S and M.G. acknowledge funding by the People Programme (Marie Curie Actions, European Union's Seventh Framework Programme FP7/2007-2013) to the Initial Training Network ZIP (Zooming In-between Plates, REA grant agreement n°604713). Discussions within ZIP stimulated this work. MS also acknowledges support by the Italian MIUR and the University of Genova. G.P. acknowledges funding of the University of Padova.

Contributions

M.S, G.P., O.P. wrote the paper. M.S, G.P., M.G. did the fieldwork, the petrographic and microstructural study. M.B. did the FE-SEM and EBSD work. O.P did the TEM work. F.N. did XRD and Raman analysis. Concept development: M.S. and G.P.

Competing financial interests

The authors declare no competing financial interests.

Figure captions

Figure 1. Pseudotachylyte in eclogitized metaperidotite. a: SEM back-scattered image of pseudotachylyte (pst) cutting across olivine (ol), which is partially replaced by antigorite (atg). Mantle plagioclase has been replaced by metamorphic garnet (grt), zoisite (zoi) and chlorite (chl). **b**: close-up of the olivine shown in (a) reveals darker relict cores of mantle olivine (ol1; #Mg = 0.89-0.91) replaced by lighter metamorphic olivine along the rim and microfractures (ol2; #Mg = 0.82-0.86).

Figure 2. Pseudotachylyte in peridotite and metagabbro. a: pseudotachylyte vein within peridotite. **b:** SEM back-scattered image showing small microlites of olivine (ol), orthopyroxene (opx; dark gray), clinopyroxene (light grey) and spinel (small bright droplets). A large olivine clast is included in the groundmass. **c**: photograph of a polished sample showing black mm-thick pseudotachylyte veins cutting eclogitic metagabbro. The igneous clinopyroxene, plagioclase and olivine in the metagabbro have been pseudomorphosed by green omphacite, white jadeite+zoisite and black chlorite+chloritoid with cores of white talc, respectively (see Supplementary Materials 1).

Figure 3. Pseudotachylyte in anhydrous gabbro. Back-scattered SEM images of Figure S6. **a**: pseudotachylyte fault (red dashed lines) cutting a gabbro preserving magmatic clinopyroxene (cpx1), olivine (ol), plagioclase (plag). Metamorphic garnet (grt) coronas formed at olivine-plagioclase boundaries close to pseudotachylyte (white arrows). Fault and associated injection vein contain pure glass layers (white dashed line) near glass layers including microlites and clasts. **b, c**: glassy pseudotachylyte hosting dendrite-like clinopyroxene microlites (cpx2; area b, plate a) with plagioclase and garnet microlites (area c,

plate a). **d**: garnet microcracks in glassy pseudotachylyte. **e:** host-rock garnet overgrowing the glassy pseudotachylyte. **f:** dendritic-like garnet in pseudotachylyte from pyroxenite.

Figure 4. Pseudotachylyte in metaperidotite-metagabbro. a: transmitted light image of pseudotachylyte (pst) at metaperidotite-metagabbro contact. In metagabbro, jadeite+zoisite (jd+zoi) replaced plagioclase, talc+chloritoid replaced olivine (ex-ol), omphacite replaced clinopyroxene (detail in (b)). In metaperidotite, metamorphic olivine (ol2) and antigorite replaced mantle olivine (ol1), garnet+zoisite+chlorite replaced plagioclase. The white arrow (rectangle b) indicates a microfault parallel to pseudotachylyte. **b**: enlarged rectangle (b). The microfault offsets cataclastic igneous clinopyroxene (cpx) cemented by omphacite (omph). **c:** SEM back-scattered image of pseudotachylyte hosting clasts of mantle ol1 overgrown by ol2. **d:** enlarged rectangle (d). Pseudotachylyte enclosing clasts of ol2+antigorite+orthopyroxene (opx) and disrupted fragments of garnet-bearing pseudomorphs after plagioclase (Fig. S8).

Figure 5. Locating seismic activity of Moncuni in a subducting slab. Seismicity in a subduction zone (modified after[42]). The brown layer corresponds to the low-velocity zone (LVZ); the light green and dark green fields represent the mantle wedge and the subducting oceanic mantle, respectively. The light grey dashed lines in the LVZ correspond to dehydration boundaries separating amphibole-lawsonite eclogite (shallow LVZ, left side), from jadeite-lawsonite eclogite (central LVZ), from anhydrous eclogite (deeper part of LVZ, right side). Circles show hypocenters in the LVZ and in the subducting plate. The star shows the interpreted location of the Moncuni seismic failure.

Methods

Moncuni samples were studied by optical and scanning electron microscope (SEM), electron microprobe, electron back scattered diffraction (EBSD) and transmission electron microscope (TEM). For SEM analysis the thin sections were SYTON-polished and carbon-coated (coating thickness of ~3.5 nm).

• Optical and Scanning electron microscopy were performed at the Universities of Genova in energy-dispersive mode with a SEM VEGA3 TESCAN operating at 15 kV and equipped with an EDAX APOLLO XSDD energy-dispersive X-ray spectrometer. Working conditions were: 15 kV accelerating potential, 20 nA beam current, 2 μm beam diameter, and 100 s counting time.

• Major element mineral compositions were analyzed by electron probe microanalysis using the JEOL 8200 Superprobe at the Dipartimento di Scienze della Terra, University of Milano. Quantitative elemental analyses were performed by wavelength-dispersive analysis at 15 kV and 60 nA. Natural silicates were used as standards. A PhiRhoZ routine was used for matrix correction. The compositions of feldspar microlites were analysed by energy dispersive X- ray spectroscopy (EDX) at the TESCAN SEM (Erlangen) equipped with the Oxford Instruments INCA system and a 50 mm^2 X-Max detector.

• Backscatter Secondary Electron (BSE) atomic Z-contrast images were collected using a ZEISS CrossBeam 1540 EsB SEM equipped with thermo-ionic field emission at the Department of Material Sciences of the University of Erlangen-Nuremberg.

• Electron Backscattered Diffraction (EBSD) analysis was performed using a ZEISS Cross-Beam 1540 EsB SEM equipped with the Oxford Instruments Channel5 EBSD system with a Norderly-II camera and Flamenco acquisition software. Working conditions were: (i) 16 mm working distance, 20 kV acceleration voltage, 120 μm aperture and high current mode resulting in ~7 nA beam current (with the ZEISS instrument).

- Focused-ion beam scanning electron microscopy and transmission electron microscopy. Electron-transparent thin foils were prepared for (scanning) transmission electron microscopy ((S)TEM) by using a FEI Talos Nanolab G3 UC focused ion beam - scanning electron microscope (FIB-SEM). FIB foils were investigated in a FEI Talos F200X (S)TEM equipped with four energy-dispersive X-ray detectors (Super-X EDX). EDX analyses of submicron-sized garnets within the pseudotachylyte were quantified using the Cliff-Lorimer method. All FIB-SEM and TEM analyses were carried out at the Microscopy Square, Utrecht University.

Data availability. Authors declare that all observations and analytical data supporting the findings of this study are available within the article and its Supplementary Information files. Mineral analyses are reported in the Supplementary Table.

References

1. Kirby, S.H., Engdahl, E. R. & Denlinger R. Intermediate-depth intraslab earthquakes and arc volcanism as physical expressions of crustal and uppermost mantle metamorphism in subducting slabs. In *Subduction: Top to Bottom, Geophys. Monogr. Ser*. **96**, G. E. Bebout et al. Eds., AGU, Washington, D. C., 195– 214, (1996).
2. Hacker, B.R., Peacock, S.M., Abers, G.A. & Holloway, S.D. Subduction factory 2. Are intermediate-depth earthquakes in subducting slabs linked to metamorphic dehydration reactions? *J. Geophys. Res*. **108,** NO. B1, 2030 (2003).
3. Frohlich, C. The nature of deep-focus earthquakes. *Ann. Rev. Earth Planet. Sci.* **17**, 227-254 (1989).
4. Abers, G.A. Seismic low-velocity layer at the top of subducting slabs: observations,

predictions, and systematics. *Phys. Earth Planet. Int.* **149**, 7–29 (2005).

5. Bostock M.G. The Moho in subduction zones. *Tectonophysics* **609,** 547–557 (2013).

6. Audet, P., Bostock, M.G., Christensen, N.I. & Peacock, S.M. Seismic evidence for overpressured subducted oceanic crust and megathrust fault sealing. *Nature* **457**, 76–78 (2009).

7. Kodaira, S. et al. High pore fluid pressure may cause silent slip in the Nankai Trough. *Science* **304**, 1295–1298 (2004).

8. Ogawa, M. Shear instability in a viscoelastic material as the cause of deep focus earthquakes. *Journal of Geophysical Research* **92**, 13801–13810 (1987).

9. Braeck, S. & Podladchikov, Y.Y. Spontaneous thermal runaway as an ultimate failure mechanism of materials. Phys. Rev. Lett. **98**, 095504 (2007).

10. Kelemen, P. B. & Hirth, G. A. Periodic shear-heating mechanism for intermediate-depth earthquakes in the mantle. *Nature* **446**, 787–790 (2007)

11. John, T. *et al.* Generation of intermediate-depth earthquakes by self-localizing thermal runaway. *Nat. Geosci.* **2**, 137–140 (2009)

12. Thielmann, M., Rozel A., Kaus, B.J.P. & Ricard, Y. Intermediate-depth earthquake generation and shear zone formation caused by grain size reduction and shear heating. *Geology* **43**, 791–794 (2015)

13. Jung, H., Green, H.W. II & Dobrzhinetskaya, L. F. Intermediate-depth earthquake faulting by dehydration embrittlement with negative volume change. *Nature* **428**, 545-549 (2004).

14. Okazaki, K. & Hirth, G. Dehydration of lawsonite could directly trigger earthquakes in subducting oceanic crust. *Nature* **530**, 81-85 (2016).

15. Green, H.W. II, Shi, F., Bozhilov, K., Xia G, & Reches Z. Phase transformation and nanometric flow cause extreme weakening during fault slip. *Nat. Geosci*. **8**, 484-490 (2015)

16. Austrheim, H. & Boundy, T.M. Pseudotachylytes generated during seismic faulting and

eclogitization of the deep crust. *Science* **265**, 82–83 (1994)

17. Austrheim, H. et al. Fragmentation of wall rock garnets during deep crustal earthquakes. *Science Advances* **3**, e1602067 (2017).

18. John, T. & Schenk, V. Interrelations between intermediate-depth earthquakes and fluid flow within subducting oceanic plates: Constraints from eclogite facies pseudotachylytes. *Geology* **34**, 557–560 (2006).

19. Austrheim, H. & Andersen, T.B. Pseudotachylytes from Corsica: Fossil earthquakes from a subduction complex. *Terra Nova* **16**, 193– 197 (2004).

20. Andersen, T.B. & Austrheim, H. Fossil earthquakes recorded by pseudotachylytes in mantle peridotite from the Alpine subduction complex of Corsica. *Earth Planet. Sci. Lett.* **242**, 58–72 (2006).

21. Deseta, N., Andersen, T.B. & Ashwal, L.D. A weakening mechanism for intermediate-depth seismicity? Detailed petrographic and microtextural observations from blueschist facies pseudotachylytes, Cape Corse, Corsica. *Tectonophysics* **610**, 138-149 (2014a).

22. Deseta, N., Ashwal, L.D. & Andersen, T.B. Initiating intermediate-depth earthquakes: Insights from a HP–LT ophiolite from Corsica. *Lithos* **206-207**, 127-146 (2014b).

23. Piccardo G.B., Ranalli, G. & Guarnieri, L. Seismogenic Shear Zones in the Lithospheric Mantle: Ultramafic Pseudotachylytes in the Lanzo Peridotite (Western Alps, NW Italy). *J. Petrol.* **51**, 81-100 (2010).

24. Piccardo, G. B., Ranalli, G., Marasco, M. & Padovano, M. Ultramafic pseudotachylytes in the Mt. Moncuni peridotite (Lanzo Massif, Western Alps): Tectonic evolution and upper mantle seismicity. *Period. Mineral.* **76**, 181-197 (2007).

25. Vitale Brovarone et al. Stacking and metamorphism of continuous segments of subducted lithosphere in a high-pressure wedge: The example of Alpine Corsica (France). *Earth Sci. Revs.* **116**, 35-56

26. Debret, B., Nicollet, C., Andreani, M., Schwartz, S., Godard, M. Three steps of serpentinization in an eclogitized oceanic serpentinization front (Lanzo Massif – Western Alps). *J. Metam. Geol.* **31**, 165-186 (2013).

27. Kienast, J.R. & Pognante, U. Chloritoid-bearing assemblages in eclogitised metagabbros of the Lanzo peridotite body (Western Italian Alps). *Lithos* **21**, 1-11 (1988).

28. Pelletier, L. & Müntener, O. High pressure metamorphism of the Lanzo peridotite and its oceanic cover, and some consequences for the Sesia-Lanzo zone (northwestern Italian Alps). *Lithos* **90**, 111-130 (2006)

29. Rubatto, D., Müntener, O., Barnhoorn, A. & Gregory, C. Dissolution-reprecipitation of zircon at low-temperature, high-pressure conditions (Lanzo Massif, Italy). *Am. Mineral.* **93**, 1519–1529 (2008).

30. Scambelluri M., Muentener O., Ottolini L., Pettke T., Vannucci R. The fate of B, Cl and Li in the subducted oceanic mantle and in the antigorite-breakdown fluids*. Earth Planet. Sci. Lett.* **222**, 217-234 (2004)

31. Lund, M.G. & Austrheim, H. High-pressure metamorphismand deep-crustal seismicity: evidence from contemporaneous formation of pseudotachylytes and eclogite facies coronas. *Tectonophysics* **372**, 59–83 (2003.)

32. Lund, M.G., Austrheim, H. & Herambert, M. Earthquakes in the deep continental crust - insights from studies on exhumed high-pressure rocks. *Geophys. J. Internat.* **158**, 569-576 (2004).

33. Abers, G. A., Nakajima, J., van Keken, P. E., Kita, S. & Hacker, B. R. Thermal– petrological controls on the location of earthquakes within subducting plates. *Earth Planet. Sci. Lett*. **369–370**, 178–187 (2013).

34. Prieto, G.A., Florez, M., & Barrett, S.A. Seismic evidence for thermal runaway during intermediate-depth earthquake rupture. *Geophys. Res. Lett.* **40**, 6064–6068 (2013).

35. Prieto, G.A., Froment, B, Yu, C. Poli, P. & Abercrombie, R. Earthquake rupture below the brittle-ductile transition in continental lithospheric mantle. *Science Advances* **3**: e1602042 (2017).

36. Andersen, T.B., Mair, K., Austrheim, H., Podladchikov, Y.Y., and Vrijmoed, J.C. Stress release in exhumed intermediate and deep earthquakes determined from ultramafic pseudotachylyte. *Geology* **36**, 995–998 (2008)

37. Dobson, D., Meredith, P. & Boon, S. Simulation of subduction zone seismicity by dehydration of serpentine. *Science* **298**, 1407-1410 (2002).

38. Gasc, J. et al. Simultaneous acousticemissions monitoring and synchrotron X-ray diffraction at high pressure and temperature: Calibration and application to serpentinite dehydration. *Phys. Earth Planet. In*. **189**, 121-133 (2011).

39. Proctor, B. & Hirth, G. Role of pore fluid pressure on transient strength changes and fabric development during serpentine dehydration at mantle conditions: Implications forsubduction-zone seismicity. *Earth Planet. Sci. Lett.* **421**, 1-12 (2015).

40. Ferrand, T. et al. Dehydration-driven stress transfer triggers intermediate-depth earthquakes. *Nature Communications* **8**, 15247 (2017).

41. Faccenda, M. & Mancktelow, N.S. Fluid flow during unbending: Implications for slab hydration, intermediate-depth earthquakes and deep fluid subduction. *Tectonophysics*, **494(1-2)**, 149-154 (2010).

42. Kita, S., Okada, T., Nakajima, J., Matsuzawa, T. & Hasegawa, A. Existence of a seismic belt in the upper plane of the double seismic zone extending in the along-arc direction at depths of 70–100 km beneath NE Japan. *Geophys. Res. Lett.* **33**, L24310 (2006).

43. Rondenay, S., Abers, G.A. & van Keken, P.E. Seismic imaging of subduction zone metamorphism. *Geology* **36**, 275–278 (2008).

44. Kawakatsu, H., Watada, S. Seismic evidence for deep-water transportation in the mantle.

Science **316**, 1468–1471 (2007).

45. Kato, A et al. Variations of fluid pressure within the subducting oceanic crust and slow earthquakes. *Geophys. Res. Lett.* **37,** (L14310) (2010).

46. Angiboust, S., Wolf, S., Burov, E., Agard, P & Yamato, P. Effect of fluid circulation on subduction interface tectonic processes: Insights from thermo-mechanical numerical modelling. *Earth Planet. Sci. Lett.* **357-358**, 238-24 (2012).

47. Ide, S., Shelly, D.R. & Beroza, G.C. The mechanism of deep low frequency earthquakes: further evidence that deep non-volcanic tremor is generated by shear slip on the plate interface. *Geophys. Res. Lett.* **34,** (L03308) (2007).

48. Faccenda, M., Burlini, L., Gerya, T. & Mainprice, D. Fault-induced seismic anisotropy by hydration in subducting oceanic plates. *Nature* **455**, 1097-1101 (2008)

49. Angiboust, S. & Agard, P. Initial water budget: The key to detaching large volumes of eclogitized oceanic crust along the subduction channel? *Lithos* **120**, 453-474 (2010).

50. Angiboust, S., Agard, P., Yamato, P. & Raimbourg, H. Eclogite breccias in a subducted ophiolite. A record of intermediate-depth earthquakes? *Geology* **40**, 707–710 (2012).

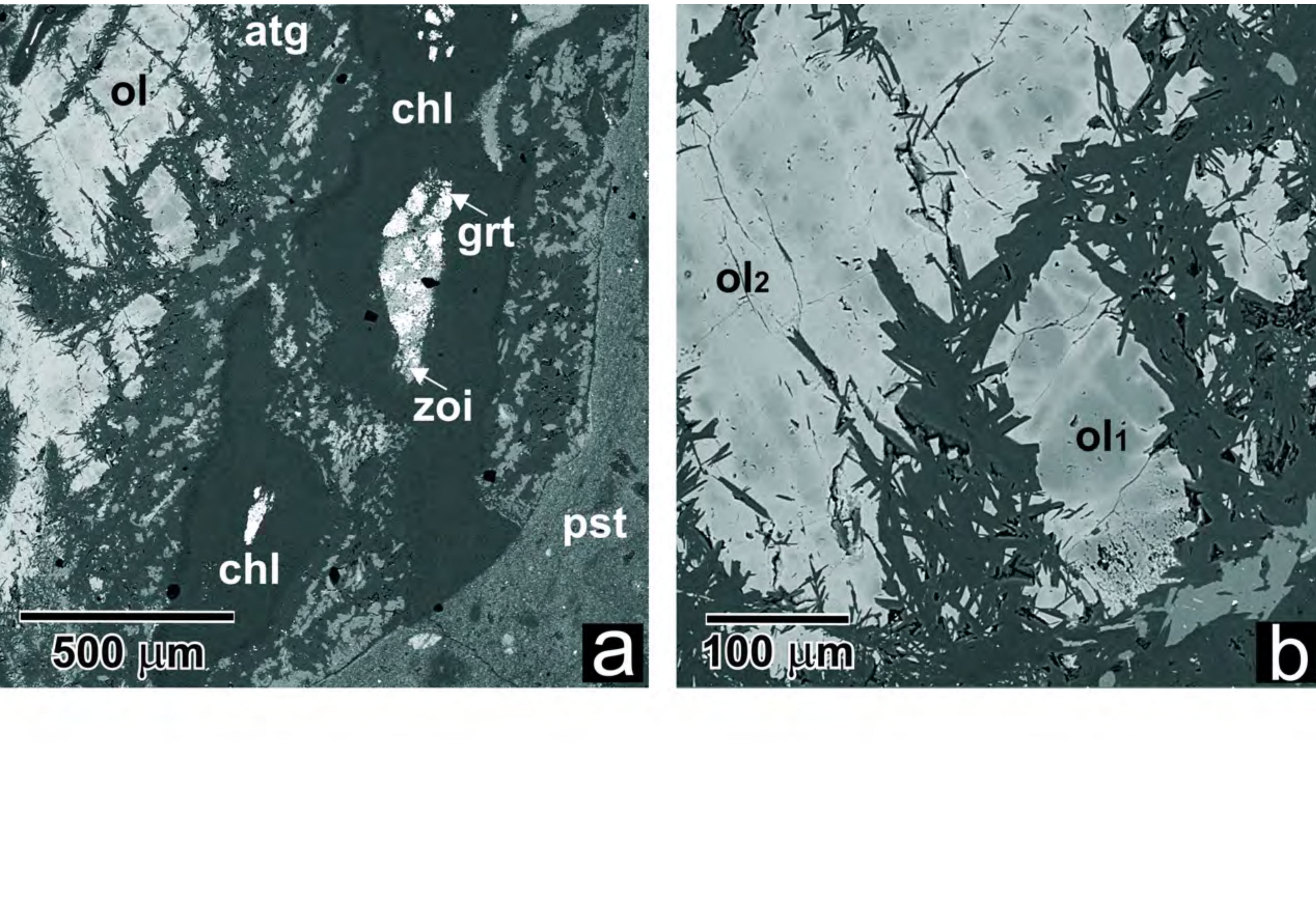
atg
ol
chl
grt
zoi
chl
pst
500 μm
a
ol2
ol1
100 μm
b

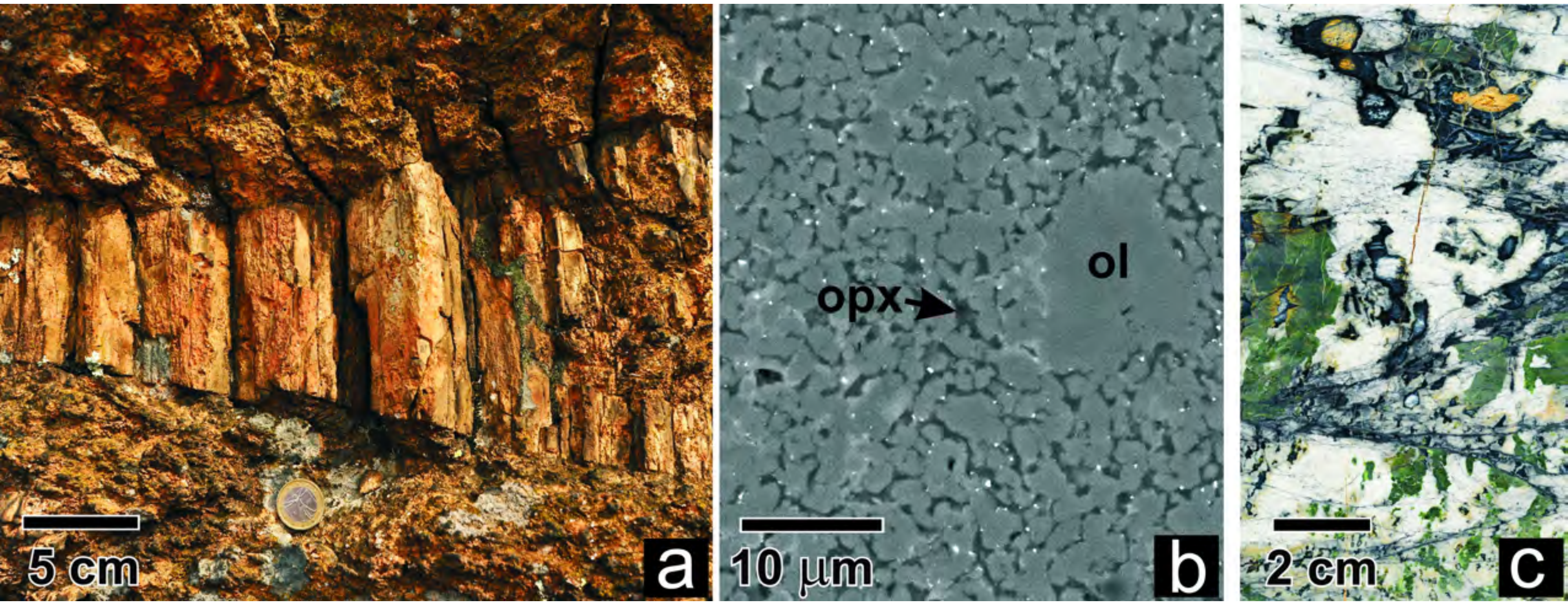
5 cm
a
opx
ol
10 μm
b
2 cm
c

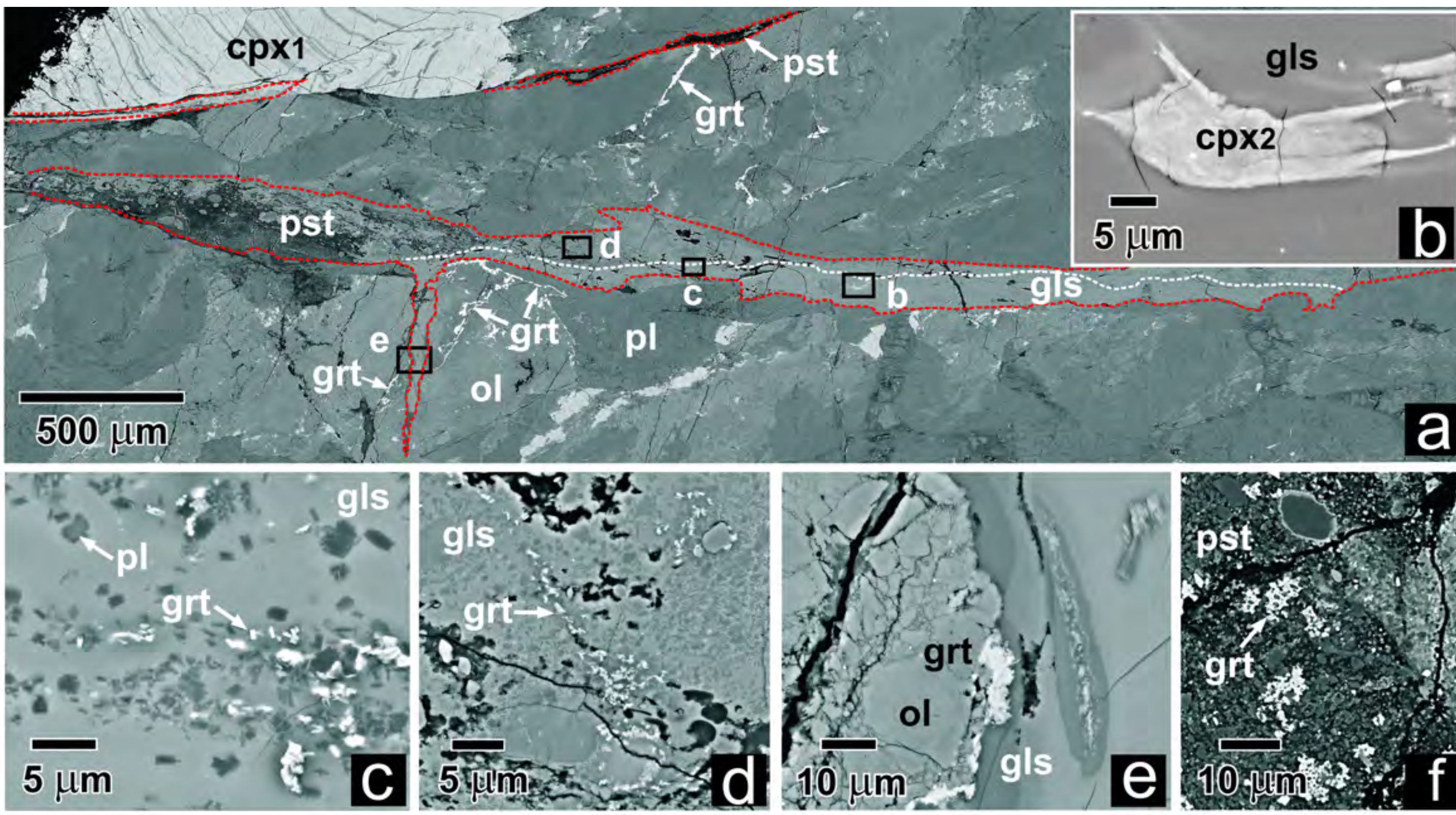

cpx1
pst
grt
pst
d
c
b
gls
e
grt
grt
pl
ol
500 µm
a
gls
cpx2
5 µm
b
gls
pl
grt
5 µm
c
gls
grt
5 µm
d
grt
ol
gls
10 µm
e
pst
grt
10 µm
f

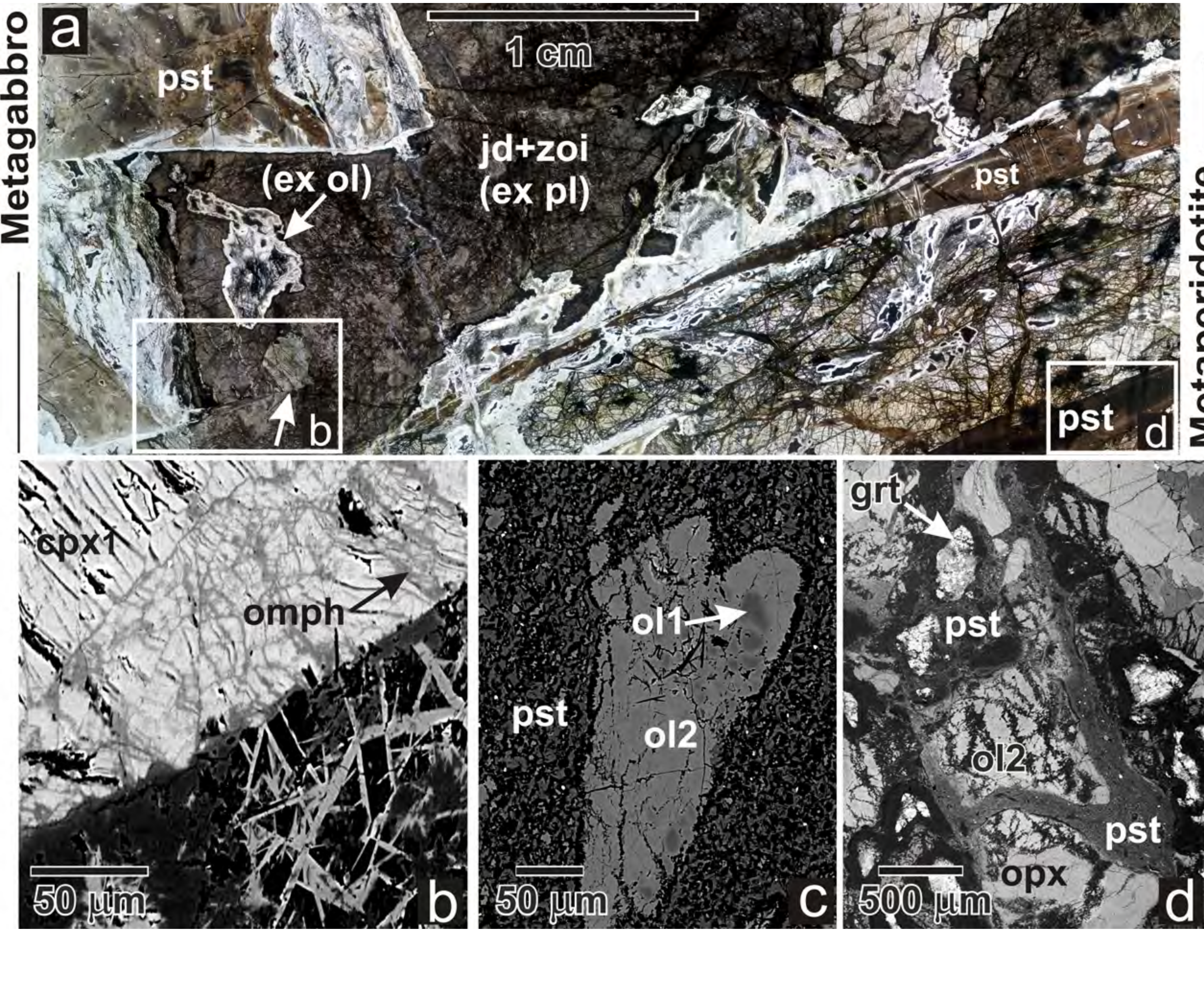

Metagabbro
Metaperidotite
a
1 cm
pst
jd+zoi
(ex pl)
(ex ol)
pst
b
pst
d
cpx1
omph
50 µm
b
ol1
pst
ol2
50 µm
c
grt
pst
ol2
pst
opx
500 µm
d

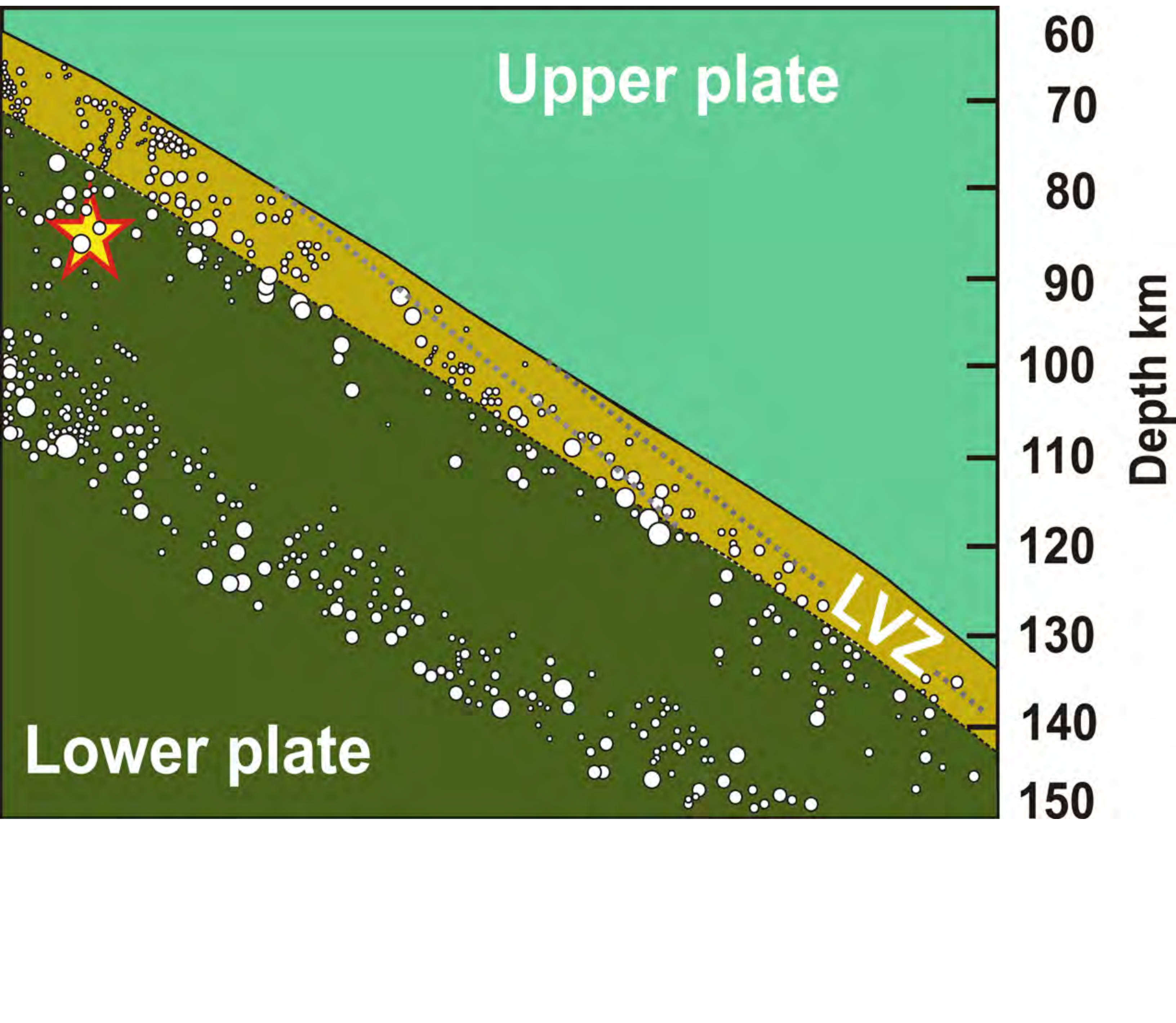

Upper plate
LVZ
Lower plate
60
70
80
90
100
110
120
130
140
150
Depth km